Current Research in Food Science 7 (2023) 100548

Contents lists available at ScienceDirect

Current Research in Food Science

journal homepage: www.sciencedirect.com/journal/current-research-in-food-science

Rapid and sensitive determination of ascorbic acid based on label-free silver triangular nanoplates

Wenteng Qiao [a,1], Yushen Liu [a,c,*,1], Xiaotong Fan [a], Yunfeng Yang [a], Wenmei Liu [a], Luliang Wang [a,c], Zhenhua Hu [a,c], Fangjie Liu [a,c], Chengwu Jin [a], Xuemei Sun [a], Daotan Liu [a], Quanwen Liu [a,**], Lin Li [b,***]

[a] College of Food Engineering, Ludong University, Yantai 264025, Shandong, China
[b] Yantai Food and Drug Inspection and Testing Center, Yantai 264035, Shandong, China
[c] Bio-Nanotechnology Research Institute, Ludong University, Yantai, 264025, Shandong, China

ARTICLE INFO

Handling Editor: Professor Aiqian Ye

Keywords:
Ascorbic acid
silver triangular nanoplates
Etching
Visualization
Colorimetric detection

ABSTRACT

In this study, a new method for the detection of ascorbic acid (AA) was proposed. It was based on the protective effect of AA on silver triangular nanoplates (Ag TNPs) against Cl^- induced etching reactions. Cl^- can attack the corners of Ag TNPs and etch them, causing a morphological shift from triangular nanoplates to nanodiscs. As a result, the solution changes color from blue to yellow. However, in the presence of AA, the corners of Ag TNPs can be protected from Cl^- etching, and the blue color of the solution remains unchanged. Using this effect, a selective sensor was designed to detect AA in the range of 0–40.00 μM with a detection limit of 2.17 μM. As the concentration of AA varies in this range, color changes from yellow to blue can be easily observed, so the designed sensor can be used for colorimetric detection. This method can be used to analyze fruit juice samples.

1. Introduction

The COVID-19 pandemic in recent years has made people pay more and more attention to their immunity. It is well known that some nutrients play a key role in maintaining the immune regulatory function of the body, such as vitamin C (ascorbic acid, AA)(Name et al., 2020). Most vitamins cannot be produced by the body or are insufficient to meet the needs of the body and must often be obtained through food. Exogenous sources of AA depend on the diet, including beverages, foods, and medications. Studies have shown that lack and excessive intake of AA were both harmful to body health(Xu et al., 2021; Zhou et al., 2023). Therefore, the accurate determination of AA was of great significance in the clinical, pharmaceutical, and food fields. Until now, common detection methods for the determination of AA in food and biological samples mainly included fluorescence(C. C. Li et al., 2023; Q. Wu et al., 2017; Zhong et al., 2022), chromatography(Abe et al., 2022; Borras et al., 2021), electrochemistry(Y. Li et al., 2022; M. Liu et al., 2013; Loguercio et al., 2022), spectrophotometry (Y. Y. Li et al., 2023; Shen et al., 2022), which have high sensitivity and specificity, but their further application was still hampered by their expensive cost, long time-consuming, intricate sample processing, and sophisticated instrument operation (Gong et al., 2017; Lihuang et al., 2019; Zhuo et al., 2019).

The colorimetric method has been well-received due to its high efficiency, simplicity, low cost, easy visual recognition, and promising application in field analysis(Y. Liu et al., 2023; T. Wu et al., 2019). Many single color detection sensors without peak spectrum change emerged as times required one after another(Y. Liu et al., 2017; Y. Liu et al., 2020). It was found that human eyes were not sensitive to the variation in light intensity of a unitary color, but tactful to the change of color with peak spectrum(de la Rica and Stevens, 2012). This urged the research of multiple color colorimetric sensors to improve the exactitude of visual detection. For example, the pH strip was the most successful multi-color sensor that quantifies hydrogen ions with the naked eye. Different concentrations of hydrogen ions correspond to different colors of pH test paper. These diverse colors greatly improved the accuracy of visual

* Corresponding author. College of Food Engineering, Ludong University, Yantai 264025, Shandong, China
** Corresponding author.
*** Corresponding author.
E-mail addresses: yushenlys@163.com (Y. Liu), liuquanwen@ldu.edu.cn (Q. Liu), 18383011@qq.com (L. Li).
[1] Contributed equally.

https://doi.org/10.1016/j.crfs.2023.100548
Received 17 April 2023; Received in revised form 1 July 2023; Accepted 9 July 2023
Available online 18 July 2023

detection and enabled people to quickly identify the pH values(Foster and Gruntfest, 1937). Regretfully, the pH dipstick only detected the concentration of hydrogen ions, so it is still challenging to use naked eyes to quantify other objects with multicolor sensors.

As a matter of fact, there are two necessary conditions for establishing a multi-color colorimetric sensor that can be distinguished by the naked eye: First, the sensor should display rich color changes so that they can be easily distinguished visually; Second, there should be a one-to-one relationship between the concentration of the analyte and the corresponding color(Ma et al., 2016). In recent years, polychromatic sensors based on gold nanorods, gold nano bipyramids, and gold nanospheres have been widely praised by researchers, while the importance of precious metal silver nanomaterials in polychromatic detection has been ignored(Hafez et al., 2021; Y. Liu et al., 2018; Y. Liu et al., 2019). Compared to gold nanomaterials, which are expensive and complex to synthesize, silver nanomaterials have become a new favorite among researchers because they provide intuitive observation, simple operation, fast procedure, and inexpensive cost (Wang et al., 2020; Yan et al., 2023; Yilmaz et al., 2021). Various optical signals were reported to be generated by controlling the directional morphology of oxidation etching, and the angle with high surface energy was the preferred corrosion site of anisotropic metal nanocrystals(H. Z. Zhang et al., 2017). Silver triangular nanoplates (Ag TNPs) stand out among many silver nanomaterials because of their unique triangular geometric anisotropy which endows them with rich optical properties. Hitherto, many polychromatic sensors based on Ag TNPs have been applied to analytical chemical detection(Kim et al., 2023; C. Zhang et al., 2021; P. Zhang et al., 2020).

As we all know, AA is a strong reducing agent and plays an important role in many chemical reactions. When the surface morphology of silver nanoparticles changes, the optical properties of silver nanoparticles change correspondingly (Rycenga et al., 2011). Using the chemical reduction of AA, silver nitrate was reduced to silver atoms and deposited on the surface of Ag TNPs, which changed the shape of Ag TNPs and produced corresponding color changes. Liu and Furletov constructed a multi-color colorimetric detection method for AA based on this principle (Furletov et al., 2022; C. Liu et al., 2021). Although this detection system has the advantages of low cost and fast response, there are still shortcomings such as low selectivity and harsh pH conditions. With the in-depth study of Ag TNPs, Ag TNPs were precisely tuned for oxidative etching after the introduction of Cl^- and produced a variety of color changes. Specifically, as the concentration of Cl^- increased, the AgTNP solution changed from blue to yellow, and the absorption peak shifted from ~600 nm to ~420 nm(Ahn et al., 2021; He and Yu, 2015). However, it has been found that DA can strongly adsorb on the surface of Ag TNPs to resist the etching effect of Cl^-. It was because that the catechol group of DA was easily adsorbed to the surface of AgNPRs through chemisorption interaction, thus avoiding the corrosion of chloride(Fang et al., 2017). Similarly, AA was found to protect Ag TNPs from Cl^- etching(Detsri et al., 2018; S. Li et al., 2019). This may be due to the fact that the dihydroxyl group on its structure makes it easy to adsorb on the surface of Ag TNPs. On this basis, we introduce a fast and sensitive Ag TNPs colorimetric sensor for the quantitative analysis of AA in food samples. Scheme 1 illustrates the experimental scheme. By exploring the influence of NaCl concentration, reaction time, pH, and other parameters, the optimal conditions were established. Under the optimal conditions, AA was detected colorimetrically using Ag TNPs in the range of 0–40.00 μM, and the detection limit was 2.17 μM. The results confirmed that our colorimetric method is sensitive, simple, and rapid for the determination of AA in fruit juice.

2. Materials and methods

2.1. Reagents and Apparatus

Silver nitrate ($AgNO_3$), Sodium chloride (NaCl), Ascorbic acid (AA), Hydrogen peroxide (H_2O_2), Sodium borohydride ($NaBH_4$), and Citric acid were purchased from Sinopharm Group Chemical Reagent Co.Ltd. (Shanghai, China). Sodium citrate dihydrate (SOD), Polyvinyl pyrrolidone (PVP), Amylaceum (Glu), Saccharose (Suc), Vitamin B_1 (VB_1), Vitamin B_6 (VB_6) were received from Shanghai Macklin Biochemical Co., Ltd. (Shanghai, China). All other chemicals and reagents used were of analytical grade.

All UV–Vis absorption spectra were obtained using Agilent Cary 60 UV–Vis (Agilent, USA). Transmission electron microscopy (TEM) of nanoparticles was measured on a JEOL JEM-2100 F transmission electron microscope at an accelerating voltage of 200 kV (JEOL, Japan).

Scheme 1. Illustration mechanism of NaCl–Ag TNPs for colorimetric sensing of AA.

2.2. Synthesis of silver triangular nanoplates (Ag TNPs)

The Ag TNPs were prepared according to the method described in the literature(Thomas and Mani, 2018).0.50 mL of silver nitrate (20.00 mM), 6.00 mL of trisodium citrate (30.00 mM), 6 mL of PVP (0.70 mM), and 240 μL H_2O_2 (30 W/W%) were mixed evenly in a volume of 144.00 mL of ultrapure water, and the mixture was stirred vigorously at room temperature for 10 min. Then, 1.00 mL of sodium borohydride (100.00 mM) prepared with fresh ice water was rapidly injected to instantly generate a light-yellow solution. After stirring for 40 min, the color of the solution gradually changed to red, green, and blue, indicating the formation of silver nanosheets.

2.3. Multicolor colorimetric detection of AA

To study the interaction between Ag TNPs and AA in the presence of NaCl, 200 μL of Ag TNPs were added to a centrifuge tube, followed by AA solutions of different concentrations (0–40.00 μM) or buffers (for the control). Next, 0.05 mL of NaCl solution (4.00 mM) was added and mixed evenly. The mixture was reacted for 7 min at room temperature. Then the color of the reaction tubes was observed with the naked eyes and the spectrum in the range of 400–800 nm was scanned with a UV–Vis spectrophotometer.

2.4. Detection of fruit juice samples

In order to evaluate the practicability of this proposed method for AA measurement in real samples, two common brands of fruit juice are selected. The sample was first filtered through a 0.22 μm microporous filter to remove insoluble components and diluted ten times with deionized water. 0.20 mL of Ag TNPs and 0.10 mL of the juice sample were mixed and finally 0.05 mL of NaCl solution (4.00 mM) was added. Then the color was observed with the naked eye, the spectrum was scanned with a UV–Vis spectrophotometer, and the recovery rate was calculated.

3. Results and discussion

3.1. Characteristics of Ag TNPs

First, $AgNO_3$ was reduced to Ag TNPs using a chemical reduction process. Here, the oxidation ability of H_2O_2 plays a crucial role in the formation of Ag TNPs, PVP as a typical surfactant has a size-limiting effect(Q. Zhang et al., 2011). The Ag TNPs were characterized by TEM, Zeta potential, UV–Vis spectroscopy, and FTIR, and the results were shown in Fig. 1. It can be seen from Fig. 1A that the prepared AgTNPs were equilateral triangles of uniform size and separated from each other. It was estimated their average edge length to be approximately 42 nm with the help of Nano Measurer (version 1.2)(Fig. 1B)(Y. Liu et al., 2017). Due to the existence of citrate in the synthesis process, the Zeta potential measurement result was −37.91 mv. Meanwhile, the optical properties of Ag TNPs were measured by UV–Vis a spectrophotometer and camera. As displayed in Fig. 1C, The absorption peak of the synthesized Ag TNPs was at 580 nm and the color of the solution was clear and transparent blue (insert). Besides, we studied the surface groups on Ag TNPs using FT-IR spectra. As demonstrated in Fig. 1D, the tensile vibration bands of Ag TNPs at 1650 cm^{-1} and 2950 cm^{-1} were enhanced, which were characteristic peaks of C═O and CH_2(Thomas et al., 2018). The band at 1443 cm^{-1} and 1074 cm^{-1} may be due to the C–O–H vibrations and C–N stretching vibrations, respectively (Vidhu et al., 2011). The above determination results proved that the triangular Ag TNPs were successfully synthesized, which laid a material foundation for the subsequent development of a colorimetric system.

3.2. Development and performance analysis of the colorimetric detection system

The detection mechanism was confirmed by photography, UV–Vis spectra, and TEM studies. It is well known that the color and absorption peak of metal nanocrystals were closely related to their morphology. It has been reported that the tips of Ag TNPs are less stable by citrate ions, and in the presence of chloride ions, the corner of Ag TNPs are better

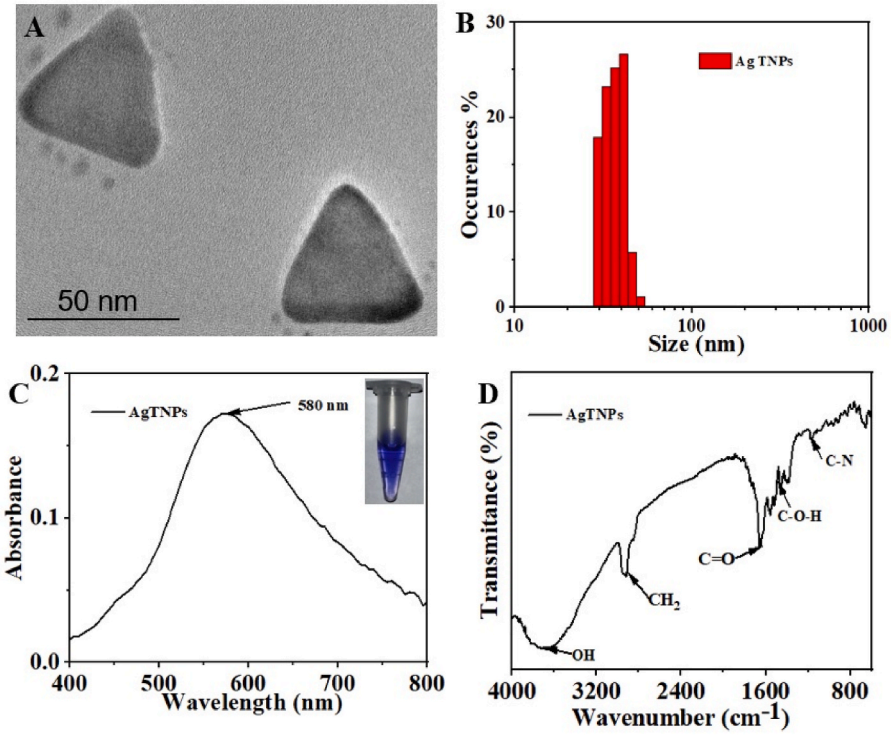

Fig. 1. A series of characterization of Ag TNPs (**A**: TEM; **B**: Histograms of the edge lengths of Ag TNPs; **C**: UV–Vis spectra; **D**: FTIR spectra).

etched(An et al., 2008). Hence, the shape transformation of Ag nanocrystals from triangles to disks leads to the color change and the shift of the absorption peak. As illustrated in Fig. 2A, the blue Ag TNPs solution turned yellow after the introduction of NaCl, but the color did not change when treated with AA. When AA and NaCl exist together, the color of the solution remains blue, suggesting that AA could inhibit the etching effect of NaCl on Ag TNPs. Fig. 2B shows the representative UV spectrum of Ag TNPs solutions treated with different substances. The absorption peak of Ag TNPs was found at 580 nm in the absence of NaCl. After the addition of NaCl, the absorption peak shifted to 460 nm and the peak intensity decreased as well. In the presence of AA, the UV spectrum was almost the same as that of solitary Ag TNPs solution, suggesting that the morphology of Ag TNPs in the solution did not change at this time. Even in the presence of NaCl, the absorption peak of the solution remained at 580 nm, which hints that the overwhelming majority of the Ag TNPs in the solution were protected by AA and no etching reaction occurred.

In order to verify the feasibility of using Ag TNPs for the naked-eye detection of AA, different concentrations of AA were selected to resist the etching effect of NaCl on Ag TNPs. Fig. 2C and D displays the typical photographs of the corresponding Ag TNPs solution after adding different amounts of AA. It was clearly shown that upon the addition of different concentrations of AA, the solution color varied from yellow, red, and violet to blue. These colors could be easily distinguished by the naked eye. Some model TEM images of Ag TNPs during etching were shown in Fig. 2D. The average edge length of the initial Ag TNPs was about 42 nm with a primary color of blue. TEM results have shown that the Ag nanocrystals in the yellow and red solutions were circular, with an average size of 18 nm and 24 nm, respectively. Most of the Ag nanocrystals in violet solutions were circular, but there were also little arc-shaped triangles with sharp corners etched, with an average size of 26 nm. A large number of triangular Ag nanocrystals were displayed in blue solutions, with sharp corners etched into circular arcs and an average side length of 31 nm. The polychromatic changes produced by Ag nanocrystals being etched into different morphologies were easily distinguished by the naked eye. It demonstrated that this method can be used for the naked-eye detection of AA.

Since many environmental factors can lead to the degradation of ascorbic acid(Gerard et al., 2019), it is necessary to explore the protective time of AA on AgTNPs to further ensure the accuracy of the detection system. Considering the degradation reaction of AA, the concentration of AA used was 50.00 μM. Other conditions were consistent with the detection system. We set up two approaches to explore the protective effect. The results were shown in Fig. S1. AA, Ag TNPs and NaCl were mixed together and placed for different time to test as group 1. After AA and Ag TNPs were attached together, the color of the experimental tube remained blue and the displacement results changed little even after 2 h. The three substances were placed at room temperature for different times and then mixed together as group 2. The results showed that the color of the experimental tube at 60min was obviously different from that of the blank group, showing a light purple color. The displacement results showed little change within 50min, and the displacement increased after 60min. We hypothesized that the cause of this result may be the degradation reaction of AA in the environment, which reduces the protective effect of AgTNPs. As for the results of group 1, it may be due to the structural changes after AA and Ag TNPs adhesion together to overcome their own unstable characteristics. Combined with the above results, it can be concluded that the detection results of AA by this detection system are reliable within 120 min, and the time process of AA being placed in the environment may affect the detection results. That's one of the reasons we're so eager to quickly detect AA.

3.3. Optimization of detection conditions

According to the principle of the polychromatic assay, the concentration of Cl^- had the most prominent effect on Ag TNPs etching. We selected four kinds of Cl^- chemicals commonly used in the laboratory to etch Ag TNPs respectively, and $NaNO_3$ as the control. The experimental results were shown in Fig. S2. Photographs and UV spectrum results demonstrated that all these Cl^- chemicals have a good etching effect on

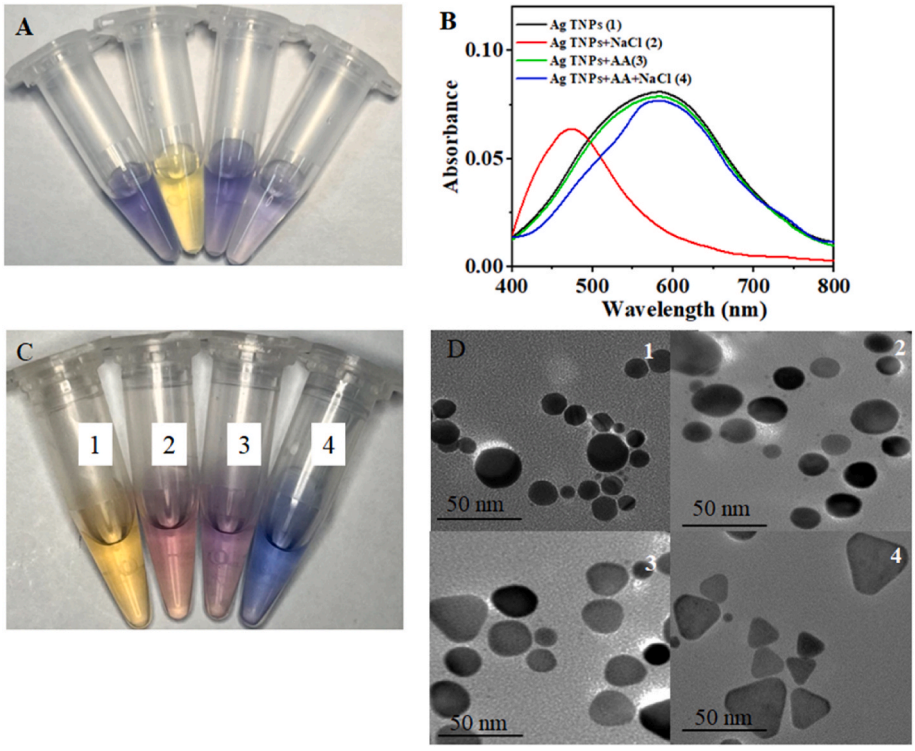

Fig. 2. Feasibility experiment. Visual (**A**) and UV–Vis spectra (**B**) of Ag TNPs under different conditions; Photographs (**C**) and TEM images(**D**) of Ag TNPs at different concentrations of AA (1: 0 μM; 2: 5 μM; 3: 15 μM; 4: 30 μM).

Ag TNPs, while the peak shift of the control group was inapparent and excluded the effect of Na^+on oxidation etching. Compared with other Cl^- chemicals, NaCl has the advantages of a cheap price, safety, and stable properties. Therefore, NaCl was selected as the etching agent for subsequent experiments. The investigation results of the etching of Ag TNPs with different concentrations of Cl^- were shown in Fig. S3A. As the concentration of Cl^- increases from 0 to 8.00 mM, the absorption peak of Ag TNPs gradually shifts blue to a shorter wavelength, and the peak shift ($\Delta\lambda$) remains almost constant when the concentration of Cl^- is greater than 4 mM. This indicated that when Cl^- concentration reached 4.00 mM, all Ag TNPs had been transformed into smaller circular disks, at which point the etching process does not continue. Finally, 4 mM was selected as the next experimental dosage.

The reaction time of the oxidative etching and AA-protected non-etching were also inspected. As can be seen from Fig. S3B, the peak shifts of NaCl and Ag NPRs in the etching reaction were gentle after 5 min. When AA was introduced, the peak shifts decreased at the same time and became stable after 7 min. This indicated that the detection could be completed within 10 min.

Next, we investigated the influence of pH and temperature on the detection system. The data results in Fig. S3C and Fig. S3D show that the peak shifts caused by these two factors are all less than 10, so the effect of these factors could be ignored. Considering the mild and easy preparation of the detection conditions, the pH of the detection system was 7 and the temperature was at room temperature for the following study.

3.4. Sensitivity of the visual detection of AA

Based on NaCl-etched Ag TNPs and their morphology-controlled color changes, a colorimetric method for the quantitative determination of AA was established. The colorimetric response of the detection system was visually discriminative and easy for quickly interpretation. Just as Fig. 3A showns, when there was no AA in the detection system, Ag TNPs were completely etched into yellow. With the increase in AA concentration, the color gradually changes to light yellow, pink, purple, and blue. When the AA concentration was 5.00 μM, the pink of the experimental group was significantly different from the yellow of 0.00 μM, so the detection limit of the naked eye was defined as 5 μM. As displayed in Fig. 3B, the absorbance peak of 4 mM NaCl etched Ag TNPs shifted by 110 nm in the absence of AA. However, with the increase of AA from 0 to 40.00 μM, the blue shifts of the absorption peak gradually decreased. When the AA concentration was 40.00 μM, the peak value almost returned to the initial Ag TNPs peak. Simultaneously, the correlation of the peak shift ($\Delta\lambda$) and AA concentration was fitted as a standard plot for determination (Fig. 3C and D). In the concentration range of 0~9 μM and 9–40 μM, the linear equation was Y = 109.84-4.36X, R^2 = 0.99, Y = 78.85-1.74X, R^2 = 0.99, where Y was the peak shift of Ag TNP, and X stood for the concentration of AA. The limit of detection for AA was 2.17 μM referring to 3σ/s. Table S1 shows several linear ranges and detection limits for different techniques used by other researchers for AA detection. Here, the colorimetric method based on NaCl-etched Ag TNPs had the advantages of easy construction, easy material access, mild reaction conditions, and lower detection limit. Compared with the previously reported method, it has a considerable linear range and detection limit.

3.5. Selectivity and interference studies

Selectivity and interference studies of this colorimetric system were investigated by 6 common substances, such as citric acid, trisodium citrate, glucose, vitamin B1, vitamin B6, and vitamin B12. In these experiments, the concentration of other species (50.00 μM) was more than one times higher than that of AA (40.00 μM). It was seen from the photograph in Fig. 4A that for except vitamin B12 shown in red, the blank and other interfering substance groups were all yellow. The blue color of the tube was consistent when AA was taken alone or in combination with other interfering substances. Fig. 4b illustrated that the peak shifts less than 20 nm in the presence of AA, while more than 100 nm were replaced by other interfering substances. In view of the fact that AA still showed good resistance to etching Ag TNPs when coexisting with other substances and vitamin B12 was very low in actual samples, we believe that this detection system has good specificity.

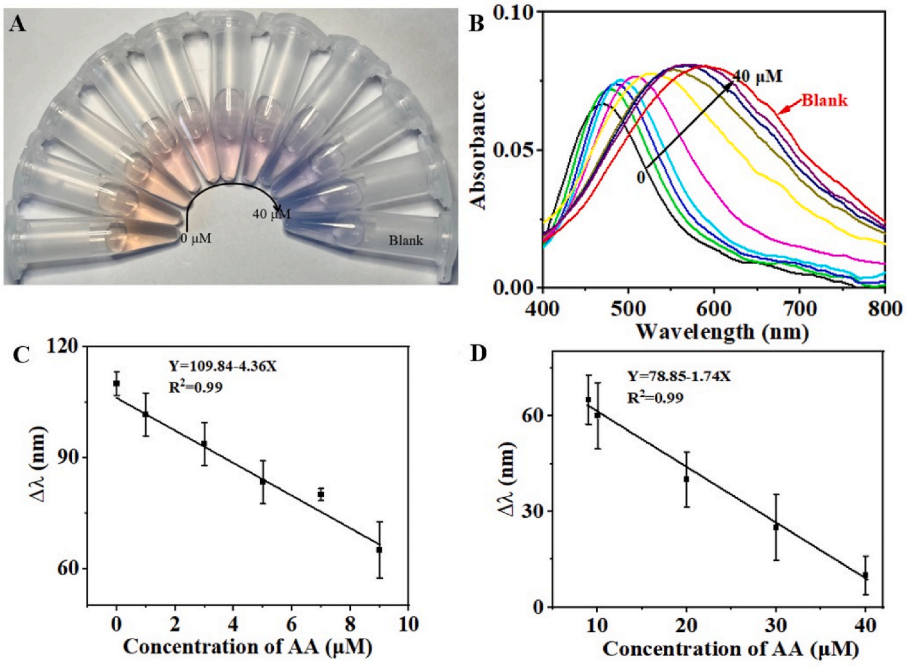

Fig. 3. Photographs (**A**) and UV–Visible spectra (**B**) of detection system after incubation with AA at various concentrations. The calibration plot (**C** and **D**) for AA (Peak shift vs. the concentration of AA). Error bars represent the standard deviation of three replicates.

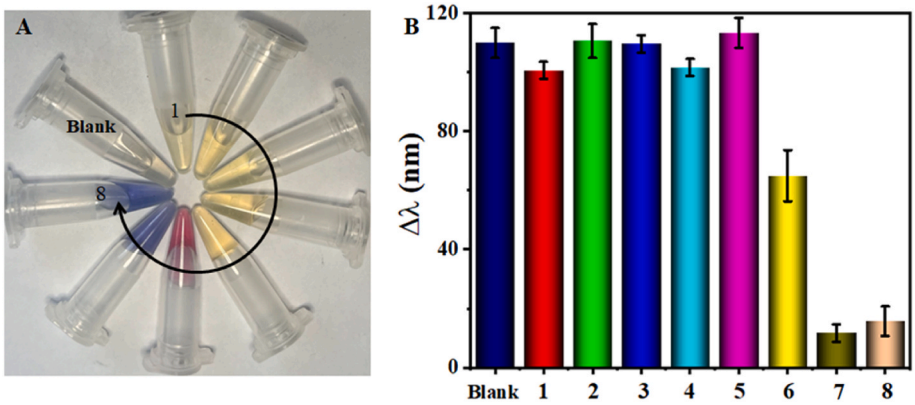

Fig. 4. Selectivity test. Photographs (**A**) of the proposed colorimetric assay in the presence of different analytes (1–8: citric acid, trisodium citrate, glucose, vitamin B1, vitamin B6, vitamin B12, AA and AA + mixture); The peak shift of the Ag TNPs in response to different analytes (**B**). Error bars represent the standard deviation of three replicates.

3.6. Quantitation of AA in fruit juice samples

To further confirm the practicability of the proposed colorimetric method, this protocol was used to detect AA in friut juice by the standard addition method. According to the ingredients list, the concentration of AA in the sample to be tested was diluted to 0.50 μM and 1.00 μM, and then a certain concentration of AA was added to calculate the recovery rate. The results obtained were summarized in Table 1. The experimental recoveries were 94.47%–105.40%. More importantly, the RSD values of the assays were 2.97%–29.94%. This result implied that the analytical method has reliable precision and accuracy.

4. Conclusions

To sum up, based on the morphology change of Ag TNPs etched with sodium chloride accompanied by color change, we have established a rapid and selective method for the detection of AA. AA can effectively inhibit the corrosion orientation morphology transformation from triangular silver nanoparticles to circular silver nanoparticles. The experimental results have shown that the preparation conditions of this colorimetric method were mild, simple, and convenient, and it has the advantages of a low detection limit, high selectivity, and good stability for AA detection. The colorimetric detection system has been successfully applied to the determination of AA in fruit juice. We believe that the strategy of controlling the etching of metal nanoparticles can be extended to other sensing systems in the future.

5. Funding information

This study was supported by the Chinese National Natural Science Foundation (Grant No. 82003502 and 21,904,053), the Science and Technology Plan Project of Yantai (Grant No. 2022XDRH004), and the Natural Science Foundation of Shandong Province (Grant No. ZR2020QB086), and the Youth Innovation Technology Project of Higher School in Shandong Province (Food Nanotechnology innovation team).

Declaration of competing interest

The authors declare that they have no known competing financial interests or personal relationships that could have appeared to influence the work reported in this paper.

Data availability

Data will be made available on request.

Table 1
The recoveries and RSD values of detecting AA in food samples ($\bar{x} \pm s$, n = 3) .

Sample	Naturally Found (μM)	Added (μM)	Calculated (μM)	Recovery rate (%)	RSD (%)
Orange juice	**(0.50)**	**1.50**	**2.11 ± 0.56**	**105.40**	**26.54**
		9.50	**9.79 ± 0.97**	**97.90**	**9.91**
		19.50	**18.89 ± 0.56**	**94.47**	**2.97**
Pineapple Juice	**(1.00)**	**4.00**	**4.95 ± 1.46**	**99.00**	**29.49**
		9.00	**10.18 ± 2.18**	**101.80**	**21.41**
		19.00	**20.07 ± 1.99**	**100.35**	**9.92**

Appendix A. Supplementary data

Supplementary data to this article can be found online at https://doi.org/10.1016/j.crfs.2023.100548.

References

Abe, C., Higuchi, O., Matsumoto, A., Miyazawa, T., 2022. Determination of intracellular ascorbic acid using tandem mass spectrometry. Analyst 147 (12), 2640–2643. https://doi.org/10.1039/d1an02160e.

Ahn, Y.J., Han, S.H., Lee, G.-J., 2021. Rapid and simple colorimetric detection of hydrogen sulfide using an etching-resistant effect on silver nanoprisms. Microchim. Acta 188 (4). https://doi.org/10.1007/s00604-021-04783-4.

An, J., Tang, B., Zheng, X., Zhou, J., Dong, F., Xu, S., Xu, W., 2008. Sculpturing effect of chloride ions in shape transformation from triangular to discal silver nanoplates. J. Phys. Chem. C 112 (39), 15176–15182. https://doi.org/10.1021/jp802694p.

Borras, E., Schrumpf, L., Stephens, N., Weimer, B.C., Davis, C.E., Schelegle, E.S., 2021. Novel LC-MS-TOF method to detect and quantify ascorbic and uric acid simultaneously in different biological matrices. J. Chromatogr., B: Anal. Technol. Biomed. Life Sci. 1168 https://doi.org/10.1016/j.jchromb.2021.122588.

de la Rica, R., Stevens, M.M., 2012. Plasmonic ELISA for the ultrasensitive detection of disease biomarkers with the naked eye. Nat. Nanotechnol. 7 (12), 821–824. https://doi.org/10.1038/NNANO.2012.186.

Detsri, E., Seeharaj, P., Sriwong, C., 2018. A sensitive and selective colorimetric sensor for reduced glutathione detection based on silver triangular nanoplates conjugated with gallic acid. COLLOIDS AND SURFACES A-PHYSICOCHEMICAL AND ENGINEERING ASPECTS 541, 36–42. https://doi.org/10.1016/j.colsurfa.2018.01.016.

Fang, X., Ren, H., Zhao, H., Li, Z., 2017. Ultrasensitive visual and colorimetric determination of dopamine based on the prevention of etching of silver nanoprisms by chloride. Microchim. Acta 184 (2), 415–421. https://doi.org/10.1007/s00604-016-2024-z.

Foster, L.S., Gruntfest, I.J., 1937. Demonstration experiments using universal indicators. J. Chem. Educ. 14 (6), 274. https://doi.org/10.1021/ed014p274.

Furletov, A.A., Apyari, V.V., Garshev, A.V., Dmitrienko, S.G., 2022. Prospects for the use of analytical systems based on silver triangular nanoplates for the spectrophotometric determination of reductants. JOURNAL OF ANALYTICAL CHEMISTRY 77 (10), 1256–1266. https://doi.org/10.1134/S1061934822100057.

Gerard, V., Ay, E., Graff, B., Morlet-Savary, F., Galopin, C., Mutilangi, W., Lalevee, J., 2019. Ascorbic acid derivatives as potential substitutes for ascorbic acid to reduce

color degradation of drinks containing ascorbic acid and anthocyanins from natural extracts. J. Agric. Food Chem. 67 (43), 12061–12071. https://doi.org/10.1021/acs.jafc.9b05049.

Gong, X., Liu, Y., Yang, Z., Shuang, S., Zhang, Z., Dong, C., 2017. An "on-off-on" fluorescent nanoprobe for recognition of chromium(VI) and ascorbic acid based on phosphorus/nitrogen dualdoped carbon quantum dot. Anal. Chim. Acta 968, 85–96. https://doi.org/10.1016/j.aca.2017.02.038.

Hafez, E., Moon, B.-S., Shaban, S.M., Pyun, D.-G., Kim, D.-H., 2021. Multicolor diagnosis of salivary alkaline phosphatase triggered by silver-coated gold nanobipyramids. Microchim. Acta 188 (12). https://doi.org/10.1007/s00604-021-05080-w.

He, Y., Yu, H., 2015. A novel triangular silver nanoprisms-based surface plasmon resonance assay for free chlorine. Analyst 140 (3), 902–906. https://doi.org/10.1039/c4an01774a.

Kim, C.-Y., Shaban, S.M., Cho, S.-Y., Kim, D.-H., 2023. Detection of periodontal disease marker with geometrical transformation of Ag nanoplates. Anal. Chem. 95 (4), 2356–2365. https://doi.org/10.1021/acs.analchem.2c04327.

Li, C., Xu, X., Wang, F., Zhao, Y., Shi, Y., Zhao, X., Liu, J., 2023. Portable smartphone platform integrated with paper strip-assisted fluorescence sensor for ultrasensitive and visual quantitation of ascorbic acid. Food Chem. 402 https://doi.org/10.1016/j.foodchem.2022.134222.

Li, S., Li, K., Li, X., Chen, Z., 2019. Colorimetric electronic tongue for rapid discrimination of antioxidants based on the oxidation etching of nanotriangular silver by metal ions. ACS APPLIED MATERIALS & INTERFACES 11 (40), 37371–37378. https://doi.org/10.1021/acsami.9b14522.

Li, Y., Javed, R., Li, R., Zhang, Y., Lang, Z., Zhao, H., Ye, D., 2023. A colorimetric smartphone-based sensor for on-site AA detection in tropical fruits using Fe-P/NC single-atom nanoenzyme. Food Chem. 406 https://doi.org/10.1016/j.foodchem.2022.135017, 135017-135017.

Li, Y., Pan, F., Yin, S., Tong, C., Zhu, R., Li, G., 2022. Nafion assisted preparation of prussian blue nanoparticles and its application in electrochemical analysis of L-ascorbic acid. Microchem. J. 177 https://doi.org/10.1016/j.microc.2022.107278.

Lihuang, Peng, Zhang, Ziyang, Danyang, Bin, Lei, 2019. CuS/Prussian blue core-shell nanohybrid as an electrochemical sensor for ascorbic acid detection. Nanotechnology 30 (32), 325501. https://doi.org/10.1088/1361-6528/ab1613.

Liu, C., Pang, Q., Wu, T., Qi, W., Fu, W., Wang, Y., 2021. A rapid visual detection of ascorbic acid through morphology transformation of silver triangular nanoplates. JOURNAL OF ANALYSIS AND TESTING 5 (3), 210–216. https://doi.org/10.1007/s41664-021-00174-z.

Liu, M., Chen, Q., Lai, C., Zhang, Y., Deng, J., Li, H., Yao, S., 2013. A double signal amplification platform for ultrasensitive and simultaneous detection of ascorbic acid, dopamine, uric acid and acetaminophen based on a nanocomposite of ferrocene thiolate stabilized Fe3O4@Au nanoparticles with graphene sheet. Biosens. Bioelectron. 48, 75–81. https://doi.org/10.1016/j.bios.2013.03.070.

Liu, Y., Sun, M., Qiao, W., Cong, S., Zhang, Y., Wang, L., Liu, Q., 2023. Multicolor colorimetric visual detection of Staphylococcus aureus based on Fe3O4-Ag-MnO2 composites nano-oxidative mimetic enzyme. Anal. Chim. Acta 1239. https://doi.org/10.1016/j.aca.2022.340654.

Liu, Y., Wang, J., Song, X., Xu, K., Chen, H., Zhao, C., Li, J., 2018. Colorimetric immunoassay for Listeria monocytogenes by using core gold nanoparticles, silver nanoclusters as oxidase mimetics, and aptamer-conjugated magnetic nanoparticles. Microchim. Acta 185 (8), 360. https://doi.org/10.1007/s00604-018-2896-1.

Liu, Y., Wang, J., Zhao, C., Guo, X., Song, X., Zhao, W., Li, J., 2019. A multicolorimetric assay for rapid detection of Listeria monocytogenes based on the etching of gold nanorods. Anal. Chim. Acta 1048, 154–160. https://doi.org/10.1016/j.aca.2018.10.020.

Liu, Y., Zhao, C., Song, X., Xu, K., Wang, J., Li, J., 2017. Colorimetric immunoassay for rapid detection of Vibrio parahaemolyticus. Microchim. Acta 184 (12), 4785–4792. https://doi.org/10.1007/s00604-017-2523-6.

Liu, Y., Zhao, C., Zhao, W., Zhang, H., Yao, S., Shi, Y., Wang, J., 2020. Multi-functional MnO2-doped Fe3O4 nanoparticles as an artificial enzyme for the colorimetric detection of bacteria. Anal. Bioanal. Chem. 412 (13), 3135–3140. https://doi.org/10.1007/s00216-020-02563-2.

Loguercio, L.F., Thesing, A., Noremberg, B.d.S., Lopes, B.V., Maron, G.K., Machado, G., Villarreal Carreno, N.L., 2022. Direct laser Writing of poly(furfuryl alcohol)/graphene oxide electrodes for electrochemical determination of ascorbic acid. Chemelectrochem 9 (17). https://doi.org/10.1002/celc.202200334.

Ma, X., Chen, Z., Kannan, P., Lin, Z., Qiu, B., Guo, L., 2016. Gold nanorods as colorful chromogenic substrates for semiquantitative detection of nucleic acids, proteins, and small molecules with the naked eye. Anal. Chem. 88 (6), 3227–3234. https://doi.org/10.1021/acs.analchem.5b04621.

Name, J.J., Souza, A.C.R., Vasconcelos, A.R., Prado, P.S., Pereira, C.P.M., 2020. Zinc, vitamin D and vitamin C: perspectives for COVID-19 with a focus on physical tissue barrier integrity. Front. Nutr. 7 https://doi.org/10.3389/fnut.2020.606398.

Rycenga, M., Cobley, C.M., Zeng, J., Li, W., Moran, C.H., Zhang, Q., Xia, Y., 2011. Controlling the synthesis and assembly of silver nanostructures for plasmonic applications. CHEMICAL REVIEWS 111 (6), 3669–3712. https://doi.org/10.1021/cr100275d.

Shen, L., Khan, M.A., Wu, X., Cai, J., Lu, T., Ning, T., Zhang, J., 2022. Fe-N-C Single-Atom Nanozymes Based Sensor Array for Dual Signal Selective Determination of Antioxidants. BIOSENSORS & BIOELECTRONICS, p. 205. https://doi.org/10.1016/j.bios.2022.114097.

Thomas, N., Mani, E., 2018. Mechanism and modeling of poly[vinylpyrrolidone] (PVP) facilitated synthesis of silver nanoplates. Phys. Chem. Chem. Phys. 20 (22), 15507–15517. https://doi.org/10.1039/c8cp01610k.

Vidhu, V.K., Aromal, S.A., Philip, D., 2011. Green synthesis of silver nanoparticles using Macrotyloma uniflorum. SPECTROCHIMICA ACTA PART A-MOLECULAR AND BIOMOLECULAR SPECTROSCOPY 83 (1), 392–397. https://doi.org/10.1016/j.saa.2011.08.051.

Wang, Z., Lu, Y., Pang, J., Sun, J., Yang, F., Li, H., Liu, Y., 2020. Iodide-assisted silver nanoplates for colorimetric determination of chromium(III) and copper(II) via an aggregation/fusion/oxidation etching strategy. Microchim. Acta 187 (1). https://doi.org/10.1007/s00604-019-3982-8.

Wu, Q., Chen, H., Fang, A., Wu, X., Liu, M., Li, H., Yao, S., 2017. Universal multifunctional nanoplatform based on target-induced in situ promoting Au seeds growth to quench fluorescence of upconversion nanoparticles. ACS Sens. 2 (12), 1805–1813. https://doi.org/10.1021/acssensors.7b00616.

Wu, T., Hou, W., Ma, Z., Liu, M., Liu, X., Zhang, Y., Yao, S., 2019. Colorimetric determination of ascorbic acid and the activity of alkaline phosphatase based on the inhibition of the peroxidase-like activity of citric acid-capped Prussian Blue nanocubes. Microchim. Acta 186 (2). https://doi.org/10.1007/s00604-018-3224-5.

Xu, Y., Li, P., Hu, X., Chen, H., Tang, Y., Zhu, Y., Yao, S., 2021. Polyoxometalate nanostructures decorated with CuO nanoparticles for sensing ascorbic acid and Fe2+ ions. ACS Appl. Nano Mater. 4 (8), 8302–8313. https://doi.org/10.1021/acsanm.1c01495.

Yan, P., Zheng, X., Liu, S., Dong, Y., Fu, T., Tian, Z., Wu, Y., 2023. Colorimetric sensor array for identification of proteins and classification of metabolic profiles under various osmolyte conditions. ACS Sens. https://doi.org/10.1021/acssensors.2c01847.

Yilmaz, D.D., Demirezen, D.A., Mihciokur, H., 2021. Colorimetric detection of mercury ion using chlorophyll functionalized green silver nanoparticles in aqueous medium. Surface. Interfac. 22 https://doi.org/10.1016/j.surfin.2020.100840.

Zhang, C., Jiang, X., Yu, F., Liu, Y., Yue, Q., Yang, P., Liu, Y., 2021. Antagonistic action regulated anti-etching colorimetric detection of thiram residue in soil based on triangular silver nanoplates. SENSORS AND ACTUATORS B-CHEMICAL 344. https://doi.org/10.1016/j.snb.2021.130304.

Zhang, H.Z., Li, R.S., Gao, P.F., Wang, N., Lei, G., Huang, C.Z., Wang, J., 2017. Real-time dark-field light scattering imaging to monitor the coupling reaction with gold nanorods as an optical probe. Nanoscale 9 (10), 3568–3575. https://doi.org/10.1039/c6nr09453h.

Zhang, P., Wang, L., Zeng, J., Tan, J., Long, Y., Wang, Y., 2020. Colorimetric captopril assay based on oxidative etching-directed morphology control of silver nanoprisms. Microchim. Acta 187 (2). https://doi.org/10.1007/s00604-019-4071-8.

Zhang, Q., Li, N., Goebl, J., Lu, Z., Yin, Y., 2011. A systematic study of the synthesis of silver nanoplates: is citrate a "magic" reagent? J. Am. Chem. Soc. 133 (46), 18931–18939. https://doi.org/10.1021/ja2080345.

Zhong, Y., Zou, Y., Yang, X., Lu, Z., Wang, D., 2022. Ascorbic acid detector based on fluorescent molybdenum disulfide quantum dots. Microchim. Acta 189 (1). https://doi.org/10.1007/s00604-021-05124-1.

Zhou, T., Zhang, T., Wang, Y., Ge, D., Chen, X., 2023. Polyoxometalate functionalizing CeO2 hollow nanospheres as enhanced oxidase mimics for ascorbic acid colorimetric sensing. SPECTROCHIMICA ACTA PART A-MOLECULAR AND BIOMOLECULAR SPECTROSCOPY 289. https://doi.org/10.1016/j.saa.2022.122219.

Zhuo, S., Jing, Li, Meng, Wang, Jing, Zhu, Changqing, Du, Jinyan, 2019. Manganese(II)-doped carbon dots as effective oxidase mimics for sensitive colorimetric determination of ascorbic acid. Mikrochim. Acta: An International Journal for Physical and Chemical Methods of Analysis 186 (12). https://doi.org/10.1007/s00604-019-3887-6.